Vibration analysis of Grundfos wastewater pump station for component optimization based on numerical models.

C. Bechtold, A. Johansen, O. Kragh, K. Hansen

Department of Materials and Production, Aalborg University
Fibigerstraede 16, DK-9220 Aalborg East, Denmark
Email: cbecht21, akjo21, oolsen18, khans18@student.aau.dk,
Web page: http://www.mechman.mp.aau.dk/

Abstract
In this project the guide claw component of a Grundfos wastewater pump station is redesigned in order to reduce the noise emitted from the station when the pump is operating. The redesign is performed based on an analysis of the pump station to determine its eigenfrequencies. The analysis is conducted using a finite element model developed in ANSYS Workbench. This model is used to construct an approximate response surface, capable of describing the eigenfrequencies of the pump station as a function of five parameterized dimensions of the guide claw. An optimization is performed on this response surface, with a goal of shifting the eigenfrequencies away from the operating frequency of the pump. A new guide claw design is developed as a result of the optimization. It is concluded, that a redesign of the guide claw, together with the shortening of the guide rail components, makes it possible to shift the eigenfrequencies an acceptable distance away from the operating frequency.

Keywords: Vibrations, Modal analysis, Parameter studies, Model verification, Optimization.

1. Introduction

Grundfos manufactures and sells pump station wells for collecting and moving wastewater. The wells come in a large range of sizes and capacities and are used for pumping sewage and wastewater in both residential, municipal and industrial settings. The wells are underground, and going down into a well to perform service on the pump can be both dangerous and costly. To avoid having to go down into the well, Grundfos uses an auto coupler allowing the pump to be installed in the station by simply lowering it onto the auto coupler from above the well. Figure 1 shows how the guide claw (2) is bolted to the pump (3), and how it hooks onto the auto coupler (1). As the pump stations are often located close to residential areas, noise is a concern when the pump is operating. It has been observed, that significant noise is emitted from the pump station, and Grundfos assumes that the noise can be reduced by redesigning the guide claw connecting the pump to the auto coupler. The aim of this project is to redesign this interface, to shift the eigenfrequencies of the pump station away from the pump operating frequency. The project aims to redesign the guide claw without the use of physical tests, and so all analysis will be performed purely through finite element analysis.

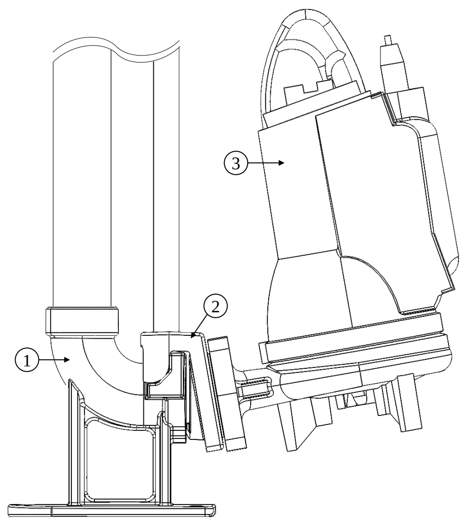

Fig. 1 Auto coupler (1) connected to pump (3) through guide claw (2). From PS.R.08.25.S.GC.304.50.A50.SEG pump station assembly. [1]

Though several pump stations exist, only a single such station is analyzed in this project. The pump station chosen in this project is the PS.R.08.25.S.GC.304.50.A50.SEG which is seen in Figure 2, henceforth called “the pump station”. The external well is excluded from all analysis, and only eigenfrequencies of the internal pipe assembly including the auto coupler, guide claw, and pump is analyzed.

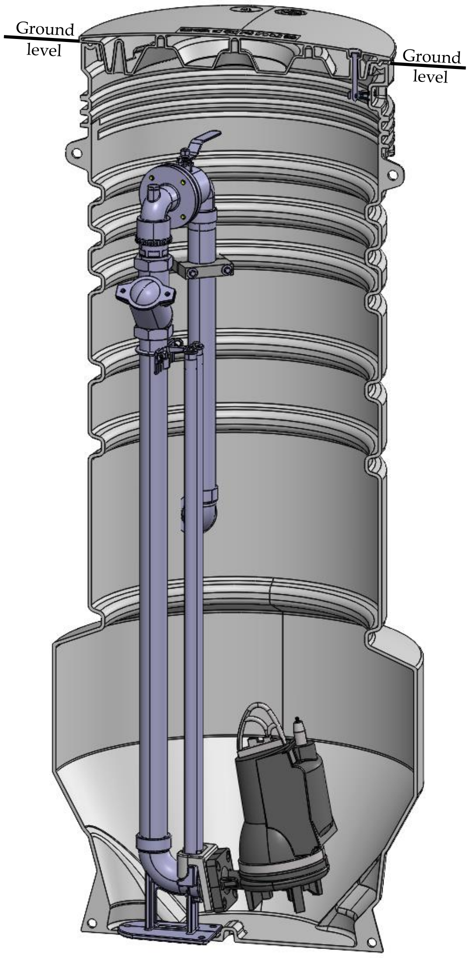

Fig. 2 PS.R.08.25.S.GC.304.50.A50.SEG pump station assembly. Only half the external well is shown for visual purposes. [1]

2. Requirements and wishes

The vibration of the pump station is assumed to originate from the pump due to an imbalance of its impeller shaft. The excitation frequency of the system is therefore assumed to be equal to the operating frequency of the pump. The impeller shaft rotates with a fixed speed of $2860\,\mathrm{RPM}$ when the pump is running, meaning the excitation frequency of the pump station is set as $f_{op} = 47.7\,\mathrm{Hz}$. Grundfos has good experience with reducing noise when moving all eigenfrequencies 20% away from the excitation frequency. It is determined, that all eigenfrequencies should lie $\geq$ 20% away from f_{op}. Based on an initial discussion with Grundfos, it is recommended to assume a 10-20% uncertainty when calculating the eigenfrequencies of the pump station using the finite element model developed in this project. An uncertainty of 20% is assumed when calculating the eigenfrequencies in this project. It is determined that for the redesign of the guide claw to be successful, no eigenfrequencies must be predicted to lie in a band between $31.8\,\mathrm{Hz}$ and $71.5\,\mathrm{Hz}$ when using the redesigned guide claw. The range between $31.8\,\mathrm{Hz}$ and $71.5\,\mathrm{Hz}$ is from now on referred to as “the critical frequency band”. Three wishes are also formulated for the redesigned guide claw:

- **Installation repeatability of pump:** Due to the way the pump is installed, it is usually not possible to visually confirm that the pump is installed correctly. The redesign of the guide claw should attempt to reduce the risk of the pump being installed incorrectly.
- **Design for simulation:** As the project is carried out without physical testing, being able to accurately simulate the true physical behavior of components is critical to producing trustworthy results. Especially the way components contact each other is difficult to simulate. The redesign of the guide claw should aim to make the contacting areas and interface effects between the auto coupler and guide claw unambiguous.
- **Castability:** The original guide claw component is produced by a sand casting of EN-GJL-250 grey cast iron. The redesigned guide claw should follow design practices for making cast components so as to not alter Grundfos’ existing production methods.

The project structure is summarized as a flowchart in Figure 3.

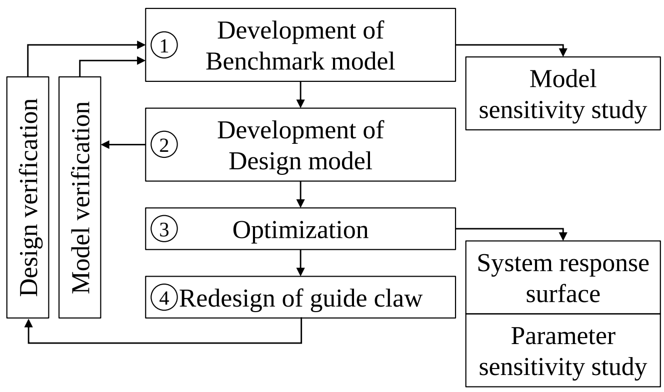

Fig. 3 Flowchart summarizing project structure.

At 1, a so-called “Benchmark model” is developed to analyze the eigenfrequencies of the pump station. Here, a study is performed to determine how model assumptions and settings affect the resulting eigenfrequencies. Next, at 2, a simplified “Design model” is developed, which is able to replicate the results from the Benchmark model, with lower solution time at the cost of model accuracy. A model verification step is performed to ensure that if a parameter is changed in both the Design model and the Benchmark model, they still predict similar results. At 3, new guide claw design concepts are developed, and parameterized CAD models of these are made. ANSYS DesignXplorer is used to produce an approximate response surface of the pump station using the new guide claw concepts. The response surface is capable of describing the eigenfrequencies of the system as a function of the parameters driving the design of the guide claw. A parameter sensitivity study is used as the basis for choosing a final guide claw concept. This chosen guide claw concept is optimized by use of the approximate response surface, and dimensions for the concept are determined. At 4, the guide claw concept is adjusted to comply with the wishes mentioned in Section 2, giving the redesigned guide claw. A final verification step is performed, in which the Benchmark model is solved using the redesigned guide claw to ensure all eigenfrequencies are predicted to lie outside the critical frequency band. This verification step will also investigate whether the redesigned guide claw will fail in static and fatigue loading.

3. Development of Benchmark model

The Benchmark model is developed in ANSYS Workbench 2022 R1 based on [2] as one-way multi-physics simulation coupling a geometrically- and contact-nonlinear structural analysis with a modal analysis. The nonlinear structural analysis provides information about how the auto coupler and guide claw contact other components when the assembly is under gravitational loading. The contact statuses and deformation calculated in the structural analysis are fed into a modal analysis and based on these, linear contact definitions are prescribed using the "use true status" setting in ANSYS Workbench. The modal analysis is then solved to obtain eigenfrequencies and mode shapes of the pump station. The Benchmark model is solved to obtain the 10 lowest eigenfrequencies, which are presented in Table I. Eigenfrequencies f_2, f_3, and f_4, indicated in grey, lie within the critical frequency band. The mode shapes associated with f_2, f_3, and f_4 are visualized in Figure 4.

Tab. I The 10 lowest eigenfrequencies calculated in the Benchmark modal analysis. Gray cells indicate the eigenfrequency lies within the critical frequency band.

f_i	Frequency [Hz]	f_i	Frequency [Hz]
1	20.3	6	84.2
2	32.9	7	86.2
3	63.6	8	89.0
4	68.1	9	101.5
5	76.8	10	116.1

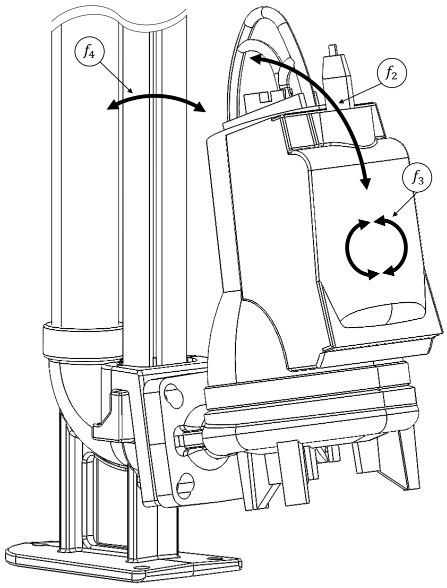

Fig. 4 Mode shapes indicated by arrows for eigenfrequencies f_2, f_3 and f_4.

In Figure 4 it is seen that f_2 is associated with a mode shape where the pump tips front to back and f_3 is associated with the pump rotating around itself together with a slight movement of the guide rails. f_4 however is almost exclusively associated with movement of the guide rails†. Analytical calculations also support the Benchmark model's prediction, of the guide rail's first eigenfrequency falling within the critical frequency band [3]. The guide rails are assumed to be simply supported in both ends, which is a slightly relaxed boundary condition, and are calculated to have a fundamental eigenfrequency of 57.9 Hz.

A sensitivity study is performed for the Benchmark model. During this it is observed that the mesh size at contacting faces between the auto coupler and guide claw affected whether sticking or sliding occurred at the contact. If sticking occurred, the first eigenfrequency would increase 17.3% compared to if sliding occurred. As the first eigenfrequency lies outside the critical

†These guide the pump and guide claw when raised and lowered.

frequency band, this does not warrant any changes to the Benchmark model. It is also observed, that the pump can be accurately modelled using a solid geometry as opposed to a fully detailed CAD model of the pump. Based on [2] the mass and center of mass position is critical to capture accurate inertia effects of the pump. The mass of the solid pump geometry is adjusted to match the fully detailed pump model by adjusting the density in the material model of the solid pump geometry. The deviation in center of mass position between the geometries is seen as negligible. It is shown that deviations in the mass moment of inertia of the pump has negligible effects on the obtained eigenfrequencies. It is also shown, that adjusting the pretension in the bolts connecting the auto coupler to the bottom of the well can affect the third eigenfrequency; increasing bolt pretension will increase the third eigenfrequency while other eigenfrequencies remained unaffected. Adjusting bolt pretensions is not investigated further as a way of moving the eigenfrequencies of the pump station outside the critical frequency band.

4. Development of Design model

The Design model is developed by performing three simplifications to the Benchmark model. These simplifications are performed to reduce the solution time of the model while attempting to keep the calculated eigenfrequencies f_1 to f_4 and their associated mode shapes unaffected. The Benchmark model has a solution time of $733\,\mathrm{s}$, which means the construction of a usable system response surface will take in the range of a week of continuous solving to complete. The system response surface must be constructible in a matter of hours, as the process includes some trial and error. The first simplification step is removing the nonlinear static structural analysis from the Benchmark model. The Design model now only contains a linear modal analysis, and contact definitions between the components in the pump station are defined manually. Appropriate contact definitions are found iteratively, being highly inspired by the contacts developed in the original Benchmark model. The first simplification results in a 96% reduction in solution time, to $\approx\ 30\,\mathrm{s}$. The resulting eigenfrequencies from simplification 1 are presented in Table II. Here it is seen that all changes in eigenfrequencies are below 5.5%. Visual inspection confirms that no visible changes occur in the associated mode shapes due to the first simplification.

Tab. II Changes in eigenfrequencies between Benchmark model and Design model due to first simplification.

Mode	Benchmark [Hz]	Simplification 1 [Hz]	Change [%]
1	20.3	21.3	+5.1
2	32.9	31.8	-3.2
3	63.3	62.9	+0.7
4	68.1	71.8	+5.5

The second simplification reduces the simulation time by reducing the number of degrees of freedom in the model. This is done by replacing all components except for the pump, auto coupler, and guide claw with beam elements. Figure 5 shows how the main pipe at 1 is replaced by beam elements with a combined length of $1200\,\mathrm{mm}$ and the same flexural rigidity as the original pipe. The two guide rails at 2 are replaced by beam elements with a combined length of $1115\,\mathrm{mm}$ each and the same flexural rigidity as the original guide rails. All three beams are constrained at the top at 3, allowing for rotation in all three directions, while constraining all translations.

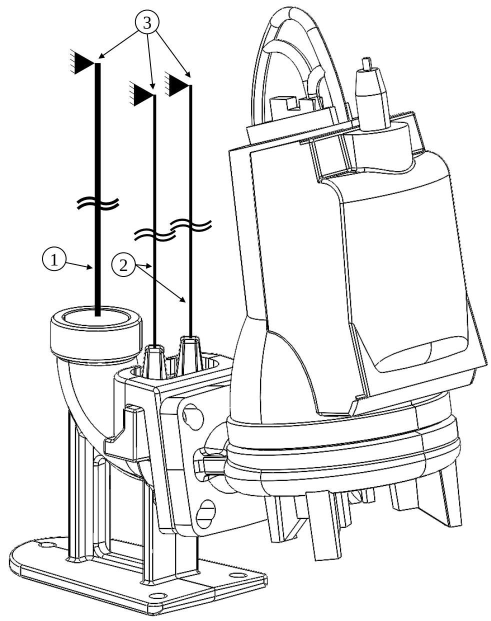

Fig. 5 Design model after the second simplification. Main pipe assembly (1) and guide rails (2) are replaced with beam elements. (3) indicates fixation allowing for rotation in all three directions, while constraining all translations.

The second simplification reduces the solution time to $25\,\mathrm{s}$, while resulting in the eigenfrequencies presented in Table III. Visual inspection confirms that no visible changes occur in the associated mode shapes due to the second simplification.

Tab. III Changes in eigenfrequencies between Benchmark model and Design model due to the second simplification.

Mode	Benchmark [Hz]	Simplification 2 [Hz]	Change [%]
1	20.3	21.6	+6.4
2	32.9	31.5	-4.3
3	63.3	65.7	+3.8
4	68.1	70.3	+3.2

The third simplification also reduces simulation time by reducing the number of degrees of freedom in the model. This is done by altering the element sizes and formulations. In the Benchmark model, the pump is meshed using $10\,\mathrm{mm}$ SOLID187 quadratic elements. Integration over the discretized volume of the pump gives a calculated mass of $49.104\,\mathrm{kg}$ which is +4 grams from the nominal mass of the pump. The mesh of the pump is changed to $20\,\mathrm{mm}$ SOLID185 linear elements. The calculated mass of the pump using the new mesh is $48.7\,\mathrm{kg}$, which is $-0.4\,\mathrm{kg}$ from the nominal mass of the pump. Though the error in mass is $\approx$ 100 times larger the gain in solution speed is valued higher than the loss of accuracy. When re-meshing the auto coupler it is observed, that a lower simulation time can be achieved using fewer higher-order elements as opposed to many lower-order elements. It is also observed, that no significant reduction in simulation time is achieved by increasing the element size of the auto coupler beyond $8\,\mathrm{mm}$, and so the element size is increased from $5\,\mathrm{mm}$ to $8\,\mathrm{mm}$ SOLID187 elements on the auto coupler.

The third simplification reduces the solution time to $12\,\mathrm{s}$ while resulting in the eigenfrequencies presented in Table IV. It is observed, that all eigenfrequencies increase, which is likely an effect of artificial stiffening from the larger discretization in the Design model. Visual inspection confirms that no visible changes occur in the associated mode shapes due to the third simplification.

Tab. IV Changes in eigenfrequencies between Benchmark model and Design model due to the third simplification.

Mode	Benchmark [Hz]	Simplification 3 [Hz]	Change [%]
1	20.3	21.9	+7.9
2	32.9	33.5	+1.8
3	63.3	66.6	+5.2
4	68.1	70.2	+3.1

As the Design model is used to describe the eigenfrequencies of the pump station when changes are made to the guide claw, a change in both the Benchmark model and Design model must result in the same change in calculated eigenfrequencies between the models. Model verification is performed, first by changing the modulus of elasticity in the material definition for the auto coupler in both models. Secondly by changing the modulus of elasticity in the material definition for the guide claw in both models. The modulus of elasticity is reduced from $110\,\mathrm{GPa}$ to $20\,\mathrm{GPa}$ in both cases. The resulting eigenfrequencies and deviations are presented in Table V. Here it is observed, that the deviations fall within $\pm 2\%$ except for two cases (marked in grey in Table V). The two large deviations are not seen as a problem, as the two models agree well in all other eigenfrequencies. Additionally, as the final guide claw design is verified using the Benchmark model in the end any erroneous predictions from the Design model are identified in this step.

Tab. V Deviation between the Benchmark model and the Design model when stiffness of guide claw and auto coupler is changed.

	Change of Guide Claw stiffness		
Mode	Benchmark [Hz]	Design [Hz]	Deviation [%]
1	15.3	15.1	-0.8
2	21.9	21.7	-1.2
3	46.5	38.3	-17.6
4	67.7	68.4	1.0
	Change of Auto Coupler stiffness		
	Benchmark [Hz]	Design [Hz]	Deviation [%]
1	12.7	11.3	-11.2
2	20.4	20.4	-0.2
3	47.5	46.7	-1.8
4	59.1	58.0	-1.9

5. Parameterization of guide claw

Three different guide claw concepts are generated, all capable of meeting the wishes presented in Section 2. The concepts are drafted in CAD, and 5 of their dimensions are parameterized. These parameters (P1 - P5) are indicated for concept 1 in Figure 6.

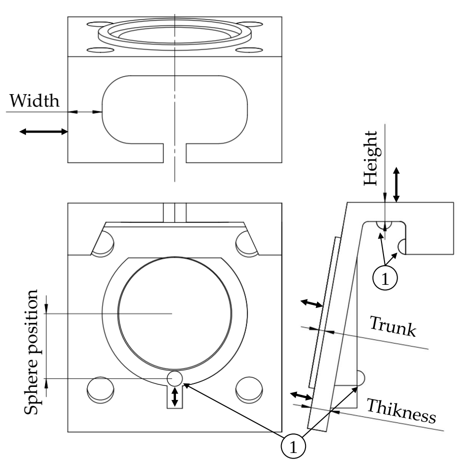

Fig. 6 Parameterized dimensions (P1 - P5) of guide claw concept 1.

The dimensions are allowed to attain any value between the limits specified in Table VI. The position of the double arrow indicates which face is extruded when the dimension is altered; the opposing face remains fixed relative to any other geometry in the guide claw. The spheres at 1 fully define the position of the guide claw on the auto coupler, and so make it unambiguous which faces should be bonded in the finite element model. Hole sizes and positions are not altered from the original guide claw in the three concepts, so as to not affect the way the guide claw is installed on the pump, or how water flows through the guide claw.

Tab. VI Limits for parameterized dimensions of guide claw concept 1.

Concept 1			
ID	Parameter	Min [mm]	Max [mm]
P1	Sphere position	26.5	40
P2	Width	17	30
P3	Height	5	30
P4	Thickness	5	30
P5	Trunk	1	30
P6	Guide rail length	900	1115

The three concepts are simulated in the Benchmark model and Design model, to verify the models gave similar results using various guide claw designs, see Table VII.

Tab. VII Comparison between Benchmark model and Design model for concept 1, 2 and 3 with all dimensional parameters set to mean values.

Concept 1			
Mode	Benchmark [Hz]	Design [Hz]	Diff. [%]
1	20.7	21.8	5.3
2	24.6	31.4	27.6
3	68.9	71.0	3.0
4	70.4	76.5	8.7
5	81.6	77.5	-5.0
Concept 2			
Mode	Benchmark [Hz]	Design [Hz]	Diff. [%]
1	14.5	16.6	14.5
2	24.9	24.3	-2.4
3	68.9	72.4	5.1
4	74.2	75.9	2.3
5	84.7	77.5	-8.5
Concept 3			
Mode	Benchmark [Hz]	Design [Hz]	Diff. [%]
1	10.2	13.4	31.4
2	24.3	24.2	-0.4
3	68.9	72.4	5.1
4	74.1	75.8	2.3
5	83.9	77.5	-7.6

Here it is observed, that the Design model generally over-predicts eigenfrequencies within the critical frequency band. It is also observed, that f_2 is over-predicted 27.6% by the Design model for concept 1. As before, this error does not warrant any changes to the Design model as the final guide claw design is verified using the Benchmark model in the end, and any erroneous predictions from the Design model are identified in this step.

During a sensitivity study of the 5 parameterized dimensions of each concept, it is concluded that concept 1 is best suited to move f_2 and f_3 outside the critical frequency band by decreasing f_2 while increasing f_3. As $f_3 \leq f_4$, shifting f_3 above the critical frequency band, will also shift f_4 sufficiently. The sphere position parameter (P1) is removed, as it has no measurable effect on the eigenfrequencies. It is observed, that f_3 is difficult to shift by changing the dimensions of concept 1. The length of the guide rails is introduced as a new parameter, $P6$ (See Table VI). This is done in an attempt to be able to shift f_3, based on the analytical calculation of eigenfrequencies of the guide rails. Their length is an easily adjustable variable affecting the eigenfrequency, and so it is introduced as a parameter. The Original guide rail length is $1115\,\mathrm{mm}$, and the parameter is allowed to attain any value between $900\,\mathrm{mm}$ and $1115\,\mathrm{mm}$.

6. Optimization

The optimization is performed using the Multi-Objective Genetic Algorithm (MOGA) [4] to obtain Pareto optimal points for minimizing f_2 while maximizing f_3 [5]. Afterward, a cost function is formulated to select a Pareto optimal solution, giving the final dimensions of the guide claw. The MOGA algorithm is presented as a block diagram in Figure 7.

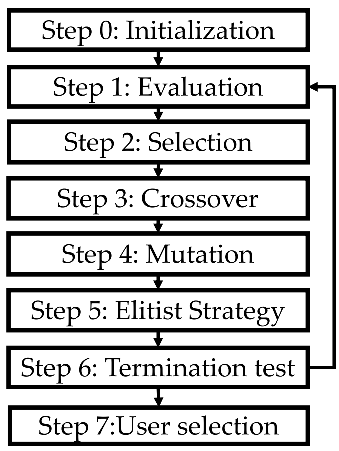

Fig. 7 MOGA block diagram.

Randomly generated designs are weighted using a fitness function, and the best designs are selected to undergo crossovers and mutations, inspired by Darwinism. The MOGA algorithm is used for multi-objective constrained optimization, as it uses a randomly weighted scalar fitness function to converge on a set of Pareto optimal solutions, as opposed to a single local extremum.

The MOGA algorithm is expected to require several thousands of function evaluations to converge. This will take in the range of weeks to solve. This is not feasible, as the optimization is associated with some trial and error, and it will likely require several attempts to obtain useful results. To circumvent the need to run the Design model several thousands of times, the optimization is performed on an approximate response surface using the MOGA algorithm.

The response surface, Ω, is developed using ANSYS DesignXplorer, and is formulated as a piecewise multilinear interpolation between discrete points $p_i = [P2_i, P3_i, P4_i, P5_i, P6_i]$ in 5D space. Each p_i defines a unique design from the parameterized dimensions presented in Table VI within the bounds specified in the table. The response surface Ω maps $\mathbb{R}^{5+} \rightarrow \mathbb{R}^{2+}$, as it reports two eigenfrequencies as a function of 5 input parameters.

$$f_2 = \Omega_2(P2, P3, P4, P5, P6)$$
$$f_3 = \Omega_3(P2, P3, P4, P5, P6)$$

The response surface is capable of describing f_2 and f_3 as a function of p_i within 4% of the Design model's predictions as specified in ANSYS DesignXplorer. The Design model is solved with varying values for p_i and interpolation between these creates the continuous definition of Ω. The values, p_i, used for interpolation are selected using a sparse grid scheme [6]. The sparse grid scheme uses a series of increasingly fine grids to select a sufficient number of evaluation points p_i[‡]. An initialization step is performed, where 11 points, $p_1 - p_{11}$, are evaluated. At p_1 each parameter assumes its mean value within the bounds in Table VI. For the remaining 10 points, $p_2 - p_{11}$, the five parameters (P2 - P6) are set to their minimum and maximum values. These points make up a full level 1 sparse grid of the parameters [6], and these are interpolated as the first iteration of the response surface, Ω^1 [7]. The level 2 sparse grid is then evaluated by the Design model, and this is compared to Ω^1. Here, it is identified which parameters are poorly represented by the response surface. Ω^2 is then developed by interpolation of the level 1 and level 2 sparse grids. The poorly represented parameters are refined using level 3 sub-grids, and these are compared to Ω^2 to identify which parameters are still poorly represented. Ω^3 is then developed by interpolating the level 1 and 2 grids together with the level 3 sub-grids. The refinement is repeated until Ω^k is accurate within 4% of the Design model. Sparse grid scheme points are visualized for two parameters in Figure 8. A level k sparse grid is made up of all $W_{i,j}$ sub-grids where $i + j \leq k$. The principles for selecting points for two parameters are extrapolated to the five-dimensional sparse grid used for the response surface.

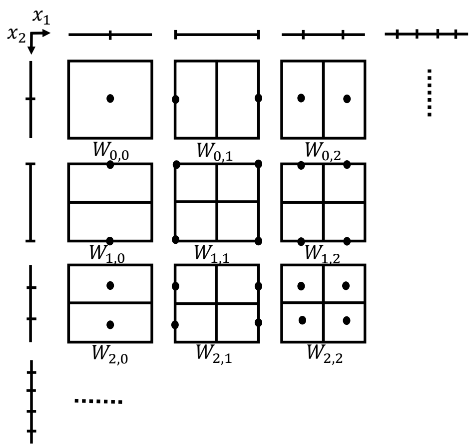

Fig. 8 Sparse grid scheme points are visualized for two parameters.

Convergence at 4% accuracy of Ω is achieved after ≈600 Design model evaluations. The MOGA algorithm identified the Pareto optimal set, Ψ, shown in Figure 9, and one of these designs are now chosen.

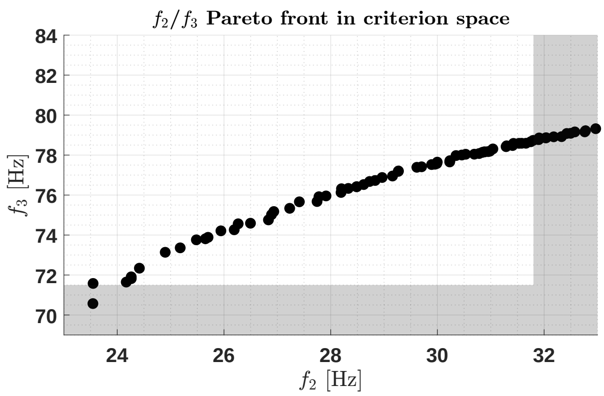

Fig. 9 f_2/f_3 Pareto front in criterion space identified by MOGA algorithm [4]. The grey area indicates critical frequency band.

‡The number of points selected is determined by the user in DesignXplorer, maximum refinement level of individual parameters or by response surface accuracy specified to 4% in this paper.

The chosen Pareto optimal solution has the largest relative distance, F, between f_2 and f_3 and the critical frequency band as described by Equation 1.

$$F = Max(G_2, G_3) \tag{1}$$

$$G_2(f_2) = \begin{cases} \frac{f_2-31.8}{31.8}, & \text{if } f_2 \leq 44 \\ \frac{71.5-f_2}{71.5}, & \text{otherwise} \end{cases}$$

$$G_3(f_3) = \begin{cases} \frac{f_3-31.8}{31.8}, & \text{if } f_3 \leq 44 \\ \frac{71.5-f_3}{71.5}, & \text{otherwise} \end{cases}$$

$$f_i \in \Psi; i = 2, 3$$

The chosen Pareto optimal solution is presented in Table VIII. All dimensions are rounded to the closest integer value. A CAD model of concept 1, see Figure 6, is generated using the parameters of Table VIII, and is called the optimized guide claw. The optimized guide claw is imported to the Benchmark model as a verification step. The Benchmark model predicts $f_2 = 26.9\,\text{Hz}$ and $f_3 = 73.6\,\text{Hz}$, indicating the optimized guide claw shifts the eigenfrequencies of the pump station outside the critical frequency band. This is however also confirmed by the Benchmark model after the guide claw has been redesigned.

Tab. VIII Dimensions for chosen Pareto optimal solution rounded to nearest integer value.

ID	Dimension $[mm]$	
P2	Width	30
P3	Height	30
P4	Thickness	24
P5	Trunk	1
P6	Guide rail length	900

7. Redesign of guide claw

The optimized guide claw is used as the basis for designing the final guide claw, to comply with the wishes in Section 2. The redesigned guide claw is presented in Figure 10, compared to the original guide claw.

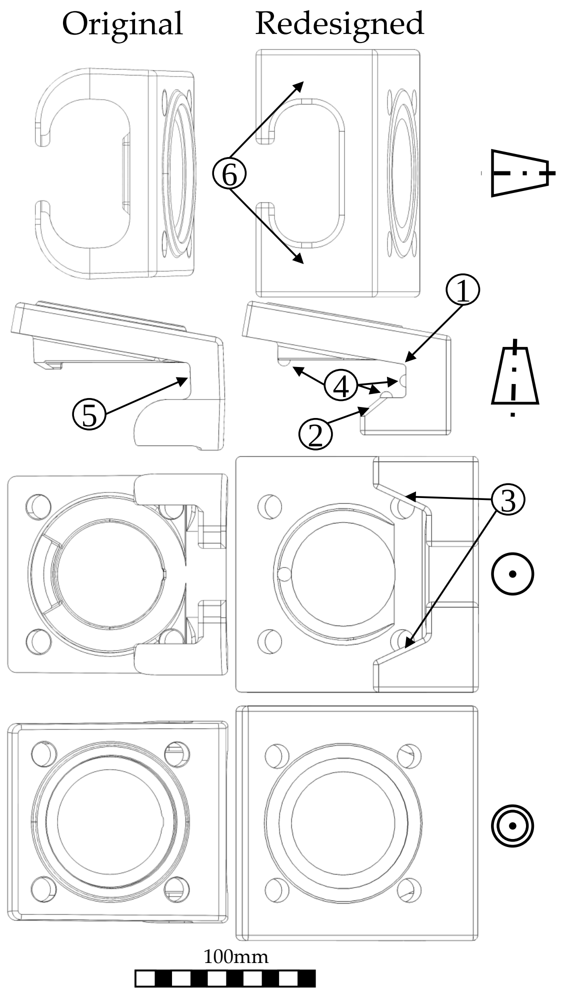

Fig. 10 Redesigned guide claw compared to original guide claw.

- **Installation repeatability of pump:** The angle the pump can be lowered, while still falling correctly into place onto the auto coupler has not been reduced by the redesign, and remains ≈ 25 degrees (See Figure 11). Large chamfers are made on any edges (2 and 3 in Figure 10) that may catch on the auto coupler during installation. It is therefore concluded that the installation repeatability is improved.
- **Design for simulation:** This redesigned guide claw uses spheres to dictate the contact points between the guide claw and the auto coupler, see 4 in Figure 10. This makes the process of defining contact sets in the Benchmark- and Design models unambiguous. The spheres are a design abstraction and should be replaced by some more easily manufacturable geometry. The final contact locations should however remain the same, and the contacting area should be kept small so as to make it unambiguous where contact occurs between the auto coupler and guide claw.
- **Castability:** The redesigned guide claw is not production-ready, and should still be seen as a concept. A prototype of the guide claw should be made for validation of its ability to reduce the noise emitted from the pump station before the redesigned guide claw is made ready for casting. The overall geometry of the redesigned guide claw is similar to the original guide claw. Because of this, it is expected, that the redesigned guide

claw can be modified to be castable, while still being able to shift the eigenfrequencies outside the critical frequency band.

During mode 2 deformation, see Figure 4, the majority of deformation in the original guide claw is associated with bending in the section indicated by 5 in Figure 10. In the redesigned guide claw, mode 2 is now primarily associated with deformation of the spheres. As the spheres take up the majority of the deformation, they reduce f_2 by decoupling the pump and guide claw from the auto coupler. In Figure 10 it is immediately obvious, that the bending stiffness and torsional rigidity have increased for the redesigned guide claw at 6. In addition to this, the guide rail length (P6) is reduced to $900\,\mathrm{mm}$ which increases their fundamental frequency. As mode 3 deformation is a combination of the pump rotating around itself deforming the guide claw, and the guide rails deforming in their fundamental mode shape, these changes effectively increase f_3.

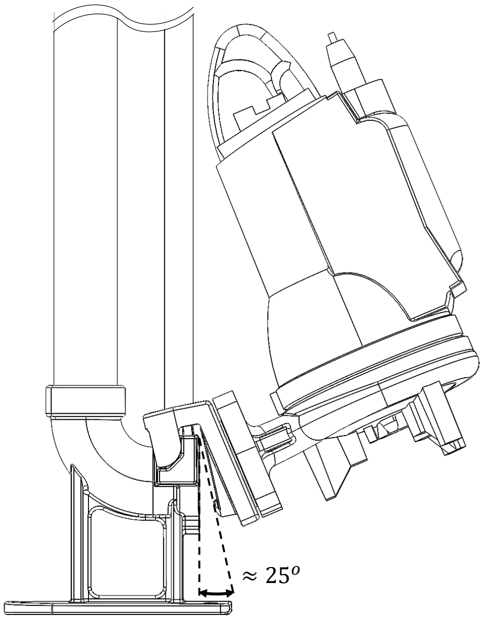

Fig. 11 Maximum angle of the pump when installed on auto coupler using original guide claw.

8. Verification of redesigned guide claw

First, it is verified, that the redesigned guide claw is able to shift the eigenfrequencies outside the critical frequency band. The Benchmark model is solved using the redesigned guide claw (see Figure 10). The resulting eigenfrequencies are tabulated together with the eigenfrequencies of the pump station using the original guide claw in Table IX. The same eigenfrequencies are presented in Figure 12. The greyed-out area in the figure indicates the critical frequency band, and the dashed line indicates the operating frequency of the pump. From the table and figure, it becomes evident, that the Benchmark model predicts that the redesigned guide claw is able to successfully shift the eigenfrequencies outside the critical frequency band.

Tab. IX Eigenfrequencies of pump station using original guide claw and redesigned guide claw.

Original		Redesigned	
f_i	Frequency [Hz]	f_i	Frequency [Hz]
1	20.3	1	23.5
2	32.9	2	26.1
3	63.6	3	73.5
4	68.1	4	75.1
5	76.8	5	95.3
6	84.2	6	109.9

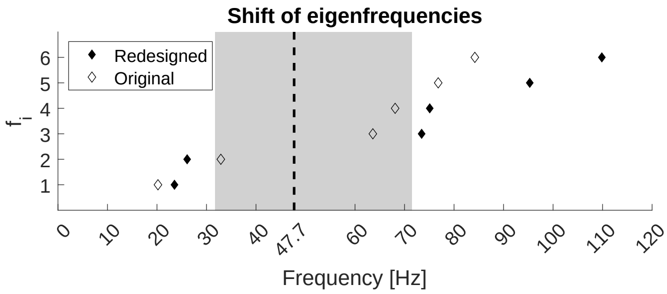

Fig. 12 Eigenfrequencies of pump station using original guide claw and redesigned guide claw. The grey area indicates the critical frequency band.

Next, the stresses developed in the guide claw are investigated to ensure it will not fail in static or dynamic loading. This is done based on the assumption, that the original guide claw designed by Grundfos, does not have stresses that will cause it to fail in static or fatigue loading. If stresses are lower or equal in magnitude for the redesigned guide claw compared to the original, it is expected to not fail in static loading. Similarly, the original guide claw has not failed in fatigue loading, and since the eigenfrequencies of the system have only been moved further away from the operating frequency, it is expected, that the cyclic loads will be lower in magnitude for the redesigned guide claw. The redesigned guide claw is made from EN-GJL-250 grey cast iron like the original guide claw. As the material has an elongation to fracture $\leq 1\%$ [8], the maximum principal stress is used as the reported stress quantity. When the dead weight of the pump is acting on the redesigned guide claw, the maximum stress is developed at 1 in Figure 10. The maximum principal stress reaches a value of $13.1\,\mathrm{MPa}$, which is far below the minimum reported tensile strength of EN-GJL-250, being $250\,\mathrm{MPa}$ [8]†. The original guide claw develops maximum principal stress at the same location as the redesigned guide claw under the same loading condition. The maximum principal stress reaches $27.4\,\mathrm{MPa}$ for the original guide claw. Based on this simple study, it is concluded, that the guide claw will likely not fail in either static or fatigue loading.

9. Conclusion

A redesigned guide claw is developed by the use of optimization. The redesigned guide claw is shown to move the eigenfrequencies outside the critical frequency band, as predicted by the Benchmark model. In addition to this, the redesigned guide claw is assumed to have improved installation repeatability compared to the original. Lastly, it is shown that the redesigned guide claw has an increased factor of safety against static failure. This, together with having moved the eigenfrequencies away from the operating frequency, is assumed to improve the factor of safety against fatigue failure.

Acknowledgement
The authors of this work gratefully acknowledge Grundfos for sponsoring the 10th MechMan symposium.

References

[1] Grundfos, "Cad model PS.R.08.20.S.GC.304.50.A50.SEG96235289," 2022.
[2] A. H. Pedersen, "Grundfos simulation procedure for fea modelling of large wastewater pumps," pp. 1–12, 2022.
[3] S.S.Rao, Mechanical Vibrations. Pearson, 5th ed., 2011.
[4] T. Murata and H. Ishibuchi, "Moga: Multi-objective genetic algorithms," 1993.
[5] J.S.ARORA, Introduction to optimum design. AP (Elsevier), 2017. Fourth Edition.
[6] D. Pflüger, "Spatially adaptive sparse grids for high-dimensional problems," Verlag Dr. Hut, 2010.
[7] I. ANSYS, "Designxplorer user's guide." Version 2021R2, 2021.
[8] COSWIG, WALZENGIESSEREI MATERIAL INFORMATION, 2022.

†Stress singularities developed around the spheres on the redesigned guide claw, but these are disregarded in the stress analysis.